© 2018. Published by The Company of Biologists Ltd | Development (2018) 145, dev161117. doi:10.1242/dev.161117

RESEARCH ARTICLE

The *Drosophila* insulin pathway controls *Profilin* expression and dynamic actin-rich protrusions during collective cell migration

Christian Ghiglione[‡,§], Patrick Jouandin[‡,*], Delphine Cérézo and Stéphane Noselli[§]

ABSTRACT

Understanding how different cell types acquire their motile behaviour is central to many normal and pathological processes. *Drosophila* border cells represent a powerful model for addressing this issue and to specifically decipher the mechanisms controlling collective cell migration. Here, we identify the *Drosophila* Insulin/Insulin-like growth factor signalling (IIS) pathway as a key regulator in controlling actin dynamics in border cells, independently of its function in growth control. Loss of IIS activity blocks the formation of actin-rich long cellular extensions that are important for the delamination and the migration of the invasive cluster. We show that IIS specifically activates the expression of the actin regulator *chickadee*, the *Drosophila* homolog of Profilin, which is essential for promoting the formation of actin extensions and migration through the egg chamber. In this process, the transcription factor FoxO acts as a repressor of *chickadee* expression. Altogether, these results show that local activation of IIS controls collective cell migration through regulation of actin homeostasis and protrusion dynamics.

KEY WORDS: *Drosophila*, Insulin pathway, FoxO, Cell migration, Actin, Profilin

INTRODUCTION

Motility of different cell types is essential for proper embryogenesis. Later during development, cell migration plays a crucial role in the immune response, during inflammation and wound-healing (Montell, 2003; Ridley, 2003). It is well established that cancer cells can re-activate embryonic migratory programs, leading to their escape from the tumour through metastasis. In all these processes, cells can migrate either alone or as cohorts; in the latter case, cells can show complex organization into mixed populations with specific functions. Cell motility can either be permanent (i.e. immune cells) or only transient, for example during an epithelial-to-mesenchymal transition or when cells re-epithelialize after reaching their target tissue. Cell migration is therefore a highly heterogeneous phenomenon that is common to both normal and pathological processes, requiring the development of genetically amenable models to identify the different molecules and signalling pathways at work.

The migration of border cells provides a unique system with which to genetically dissect the mechanisms regulating invasive cell migration *in vivo* (Montell, 2006; Rorth, 2009). Border cells are a group of about eight somatic cells composed of two central polar cells and six to eight surrounding outer border cells (Montell et al., 1992). At stage 9 of oogenesis, border cells form a cohesive cluster that undergoes an epithelial-to-mesenchymal transition, leading to its delamination from the surrounding epithelium and its posterior-ward migration through the egg chamber (Fulga and Rørth, 2002) (Fig. 1A).

Genetic as well as genome-wide profiling studies (Borghese et al., 2006; Wang et al., 2006) have identified several signalling pathways controlling distinct processes involved in border cell assembly and/or migration: whereas the early specification of pre-migratory cells requires JAK/STAT signalling and its target gene *slow border cell* (*slbo*) (Beccari et al., 2002; Devergne et al., 2007; Ghiglione et al., 2002, 2008; Silver and Montell, 2001; Van de Bor et al., 2011), the timing and guiding of cell migration depend on Ecdysone signalling (Jang et al., 2009) and PVR/EGFR pathways, respectively (Duchek and Rorth, 2001; Duchek et al., 2001; McDonald et al., 2006).

Migration of border cells is initiated by the formation of a single actin-rich 'long cellular extension' (LCE) that enables motility through a 'grapple and pull' mechanism (Fulga and Rørth, 2002). Additionally, in the course of their migration, border cells extend and retract actin-rich protrusions dynamically through cycles of F-actin assembly and disassembly (Prasad and Montell, 2007). During this 'treadmilling' process, the dynamic actin cytoskeleton is regulated by a number of molecules, including highly conserved actin-monomer-binding proteins such as Profilin, which promotes actin polymerization, and Cofilin, which enhances filament depolymerization. Mutations in these two actin-regulating proteins lead to border cell migration defects (Verheyen and Cooley, 1994). Membrane ruffling and actin protrusions are therefore important for border cell migration; however, how exactly actin dynamics is controlled in border cells to drive cell locomotion is still not fully understood.

In this study, we identify the *Drosophila* Insulin/Insulin-like growth factor signalling (IIS) pathway as an important new regulator of border cell migration. The IIS pathway couples growth with nutrition (Andersen et al., 2013; Edgar, 2006), and, during oogenesis, it has been shown to regulate germline stem cell division, cyst growth, vitellogenesis and epithelial cell cycle progression (Drummond-Barbosa and Spradling, 2001; Jouandin et al., 2014; LaFever, 2005; LaFever et al., 2010). Here, we show that specific loss of IIS activity in border cells leads to an immotile phenotype. Our results show that the function of IIS in border cells is independent of its role on cell growth control. We reveal that activation of the *Drosophila* Insulin Receptor at the onset of migration relieves the repressive activity of FoxO on the *Drosophila* Profilin-encoding gene *chickadee* (*chic*), therefore promoting actin polymerization and the formation of protrusions that are essential to initiate and support migration. These results demonstrate that the IIS pathway controls local cell migration through the regulation of dynamic, actin-rich protrusions.

Université Côte d'Azur, CNRS, Inserm, Institut de Biologie Valrose, Nice 06108, France.
*Present address: Harvard Medical School, Department of Genetics, Boston, MA 02215, USA.
‡These authors contributed equally to this work

§Authors for correspondence (ghiglion@unice.fr; noselli@unice.fr)

S.N., 0000-0002-7296-324X

Received 6 November 2017; Accepted 26 June 2018

Development (2018) 145, dev161117. doi:10.1242/dev.161117

RESULTS

The *Drosophila* Insulin Receptor controls border cell migration

To identify new genes involved in border cell migration, we performed an RNAi-based screen using available collections of *UAS-RNAi* transgenic flies (see Materials and Methods; C.G., D.C. and S.N. unpublished). RNAi lines were individually crossed to a composite Gal4-expressing strain (*USG>*), carrying both the *upd-Gal4* (*UPD>*; polar cell driver) and *slbo-Gal4* (*SLBO>*; outer border cell driver) drivers, therefore targeting the expression of *UAS-RNAi* constructs in both polar and outer border cells (Fig. 1A′). This combination of Gal4 lines allows the targeting of all cell types that make up the border cell cluster.

Among the candidate lines identified by this screen, the RNAi construct targeting the unique *Drosophila* Insulin Receptor (InR) (Fernandez-Almonacid and Rosen, 1987; Petruzzelli et al., 1986) led to strong defects in border cell migration. Border cell clusters from *USG>inr-RNAi* stage 10 egg chambers were not migrating (about 75%) or migrated only partially (about 15%) (Fig. 1B,C). In addition, we found that the frequency and the severity of border cell migration defects were aggravated in a inr^{ex15} (an amorphic allele for *inr*) heterozygous mutant background (*USG>inr-RNAi;* inr^{ex15}/+), with the proportion of clusters not migrating rising from 75% to 95% (Fig. 1C).

These results were confirmed by generating mosaic clones for inr^{ex15} (see Materials and Methods) (Xu and Rubin, 1993), which led to mutant clusters failing to migrate (Fig. 1E, compare with D). Detailed analysis showed that migration was blocked when outer border cells were mutant for *inr* (Fig. 1G), while clusters with only mutant polar cells migrated normally (Fig. 1H). This suggests that *inr* does not play a role in polar cells for border cell migration. These results were further confirmed by selectively expressing *inr-RNAi* in either outer border cells (using *SLBO>*) or polar cells (using *UPD>*) (Fig. 1C).

To rule out any indirect effect of *inr* depletion on border cell differentiation, we stained mosaic inr^{ex15} clusters with the two well-established border cell fate markers Slbo and Singed, and found that mutant border cells were specified normally (Fig. 1D-F; Fig. S1). Altogether, these results indicate that InR is required specifically in outer border cells for normal migration of the cluster.

The canonical IIS pathway is required for border cell migration

Signalling downstream of the *Drosophila* Insulin Receptor involves Chico (the *Drosophila* homolog of vertebrate insulin receptor substrate), PI3K and AKT, which lead to the phosphorylation and subsequent repression, through cytoplasmic retention, of the Forkhead transcription factor FoxO (Puig et al., 2003).

Expression of *chico-RNAi* in BCs using the *USG>* driver led to impaired border cell migration (Fig. 2A), consistent with our InR genetic analysis (see above). However, it has been reported that targeted expression of a dominant-negative form of the PI3K catalytic subunit ($dp110^{D945A}$) using the *SLBO>* driver has no effect on border cell migration (Duchek and Rorth, 2001; Fulga and Rørth, 2002). We repeated this experiment using *USG>* and obtained the same result (data not shown). Thus, our identification of InR and *chico* requirement was surprising and suggested that InR may act in a non-canonical pathway to control migration. To test this hypothesis further, we first analysed whether a constitutively activated form of PI3K (PI3K*, $dp110^{CAAX}$) could suppress *inr-RNAi* border cell migration defects. Expression of PI3K* rescued the *inr-RNAi* migration phenotype (Fig. 2A), indicating that InR signals through PI3K during border cell migration. In addition, expression of either P60 (a PI3K regulatory subunit whose overexpression dominantly blocks PI3K; Weinkove et al., 1999) or the inhibitory phosphatase PTEN led to severe migration phenotypes (Fig. 2A,B). Finally, generation of mutant mosaic clusters for the $dp110^{1C1}$ amorphic allele or for the akt^{1} allele and expression of *akt-RNAi* led to impaired border cell migration (Fig. 2A,C,D). These results therefore indicate that PI3K is involved in border cell migration. The discrepancy with previous results (Duchek and Rorth, 2001; Fulga and Rørth, 2002) is likely due to a poor efficiency of the $dp110^{D945A}$ construct in blocking PI3K activity when driven by *SLBO>*. Consistently, we observed weak but significant migration defects when $dp110^{D945A}$ was expressed using a stronger Gal4 driver (*C306>*; data not shown).

To further assess the role of the IIS pathway in border cell migration, we monitored the intracellular localization of the *tGPH* reporter gene (a GFP fused to the PH domain, binding to phosphoinositides) (Britton et al., 2002). In wild-type egg chambers, GPH is localized to the membranes of all the germ and follicle cells, with a stronger accumulation in germ cells (Fig. 2E) (Fulga and Rørth, 2002). We noticed a clear increase in GPH membrane localization in border cells compared with other follicle cells, starting at around stage 8-9 and persisting during cell migration, indicating higher activation of the IIS pathway in border cells (Fig. 2E-E″″).

This GPH expression pattern suggested that the IIS pathway is required in border cells both to initiate the detachment from the follicular epithelium and also during their migration. To test this hypothesis further, we took advantage of the temperature-inducible tub-Gal80^{ts}/Gal4 TARGET system (McGuire, 2003) (see Materials and Methods) to turn on the expression of P60 in border cells after they initiated their migration. Time-controlled conditional expression of P60 led to 47% of stage 10 egg chambers showing partial border cell migration compared with 7% in the absence of induction (Fig. 2F). Altogether, these results indicate that the canonical InR/Chico/PI3K/dAKT signalling pathway is required both for the detachment of the border cell cluster and throughout migration.

The IIS pathway controls F-actin levels and dynamics of cell protrusions

Border cells initiate their migration through the formation of a single long cellular extension (LCE) that promotes movement through a ‘grapple and pull’ mechanism (Fulga and Rørth, 2002). Because border cells mutant for the IIS pathway stall before they initiate migration, we tested a possible role of IIS in LCE formation on fixed tissues, using a *lacZ* reporter whose expression is under the control of the *slbo* regulatory region (*slbo-lacZ*) (Fulga and Rørth, 2002). At early stage 9, we observed cytoplasmic extensions in about 65% of the control clusters (Fig. 3A,E), with an average size of 11.5 µm (Fig. 3F), as previously reported (Colombié et al., 2017). Interestingly, inhibiting IIS through overexpression of P60 led to a reduction in the number and size of cytoplasmic extensions: only about 20% of early stage 9 clusters had an LCE (Fig. 3B,E), the size of which was much shorter with an average length of 3.9 µm (Fig. 3F). Furthermore, among the occasional P60-expressing clusters able to partially migrate, we observed that the protrusions were shorter and less frequent when compared with control (Fig. 3C,D).

To better assess the function of the IIS pathway in protrusion dynamics during border cell migration, we performed live time-lapse imaging of egg chambers in culture, with border cell clusters expressing mCD8::GFP, as previously described (Prasad and Montell, 2007). In most live control egg chambers (71%), border

Development (2018) 145, dev161117. doi:10.1242/dev.161117

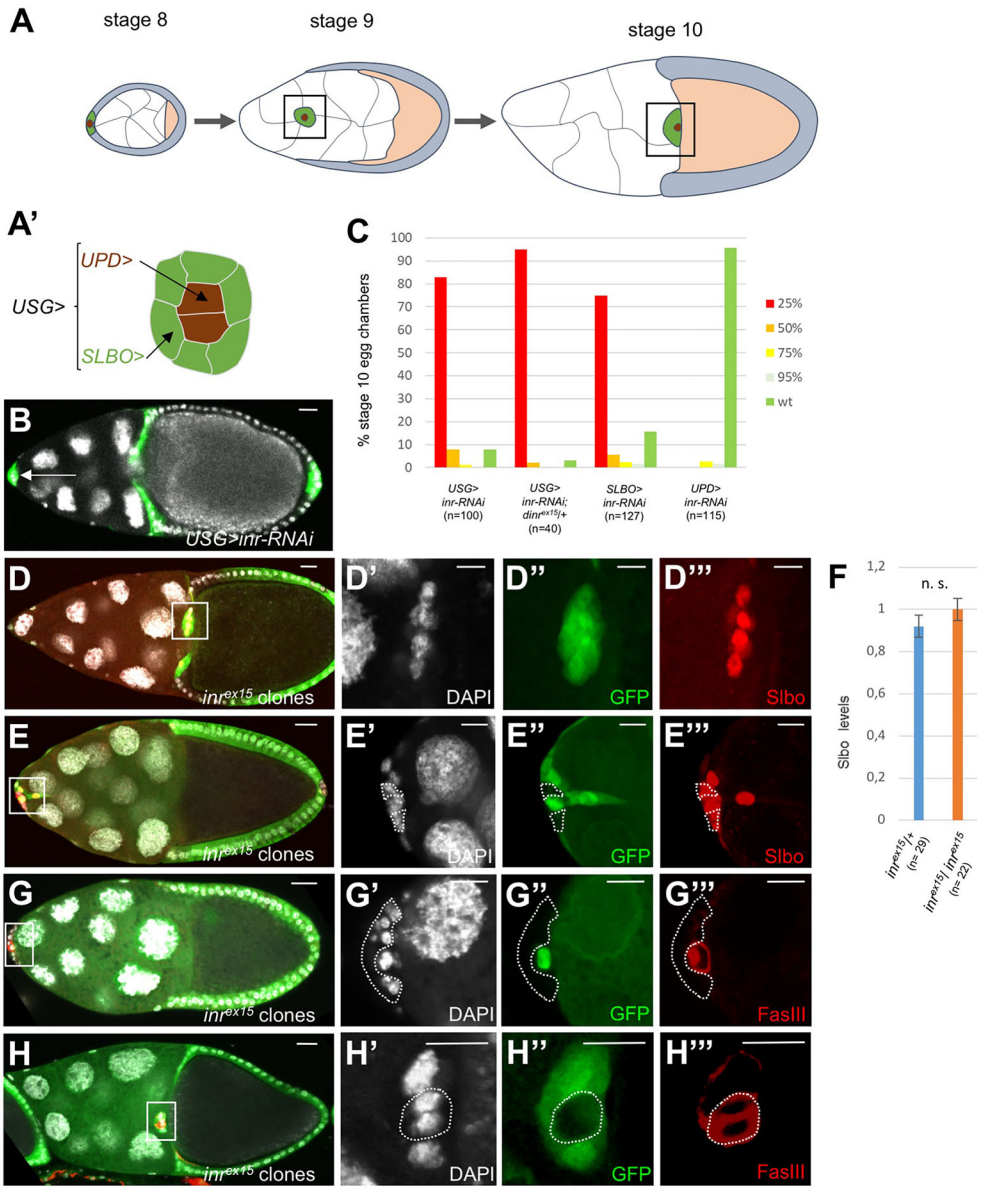

Fig. 1. The *Drosophila* Insulin Receptor is required for border cell migration. (A) Schematic representation of egg chambers (stage 8 to stage 10) showing border cell migration. Outer border cells (green) are recruited from the follicular cell epithelium (grey) by the two anterior polar cells (brown) at stage 8, to form the border cell cluster undergoing migration through the nurse cells (white) during stage 9, reaching the oocyte (orange) at stage 10. (A′) Schematic representation of a border cell cluster, composed of two central polar cells (brown) and outer border cells (green). *upd-Gal4* (*UPD>*) and *slbo-Gal4* (*SLBO>*) are polar cell and outer border cell drivers, respectively. *USG>* is a combination of these two drivers, which allows the targeting of all cells making the border cell cluster. (B) *USG>inr-RNAi* stage 10B egg chamber showing an absence of border cell migration (border cells indicated by a white arrow). *inr-RNAi*-expressing cells were identified by the presence of GFP (green). (C) Quantification of stage 10 border cell migration defects for each indicated genotype (classified as quartiles: 25%, clusters that have migrated to up to 25% of the distance; 50%, clusters that have migrated between 26 and 50% of the distance; 75%, clusters that have migrated between 51 and 75% of the distance; 95%, clusters that have migrated between 76 and 95% of the distance; wt, clusters that have reached the oocyte). (D-D′″) Expression of Slbo (red) in a control border cell cluster (stage 10B). White box in D outlines the border cells that are shown in D′-D′″. (E-E′″) Detail of a mosaic *inr*^{ex15} border cell cluster showing normal Slbo expression (red) in mutant cells (stage 10A). White box in E outlines the border cells that are shown in E′-E′″. (F) Quantification of the Slbo signal in control and *inr*^{ex15} mutant border cells. Error bars indicate s.e.m. n.s., not significant. (G-G′″) A mosaic cluster made of *inr*^{ex15} mutant outer border cells and wild-type polar cells (indicated by Fas III, in red) remained attached to the anterior tip of the late stage 9-early stage 10 egg chamber. White box in G outlines the border cells that are shown in G′-G′″. (H-H′″) A mosaic cluster made of *inr*^{ex15} mutant polar cells (indicated by Fas III, in red) and wild-type outer border cells migrated normally (stage 10B). White box in H outlines the border cells that are shown in H′-H′″. (D-H) *inr*^{ex15} mutant cells were identified by the absence of GFP and are outlined with white dotted lines. (B-H) Nuclei are labelled using DAPI (grey). GFP (green) is used as a clonal marker. Slbo (D-E′″) and FasIII (G-H′″) are shown in red. Scale bars: 20 µm in B-H; 10 µm in D′-H′″.

cells extended protrusions in the direction of migration, delaminated from the follicular epithelium around late stage 8/early stage 9, and migrated towards the oocyte over the course of 4-6 h (Movie 1). In contrast, expression of P60 (Movie 2) or FoxO (Movie 3) strongly inhibited border cell delamination and migration. Indeed, although cluster formation was normal, 83% of P60 and 80% of FoxO-expressing clusters had not yet delaminated at stage 10 (Movies 2 and 3). Notably, some occasional P60- or FoxO-expressing clusters were able to delaminate, allowing us to determine their migration speed. Whereas control clusters migrated at an average speed of

Development (2018) 145, dev161117. doi:10.1242/dev.161117

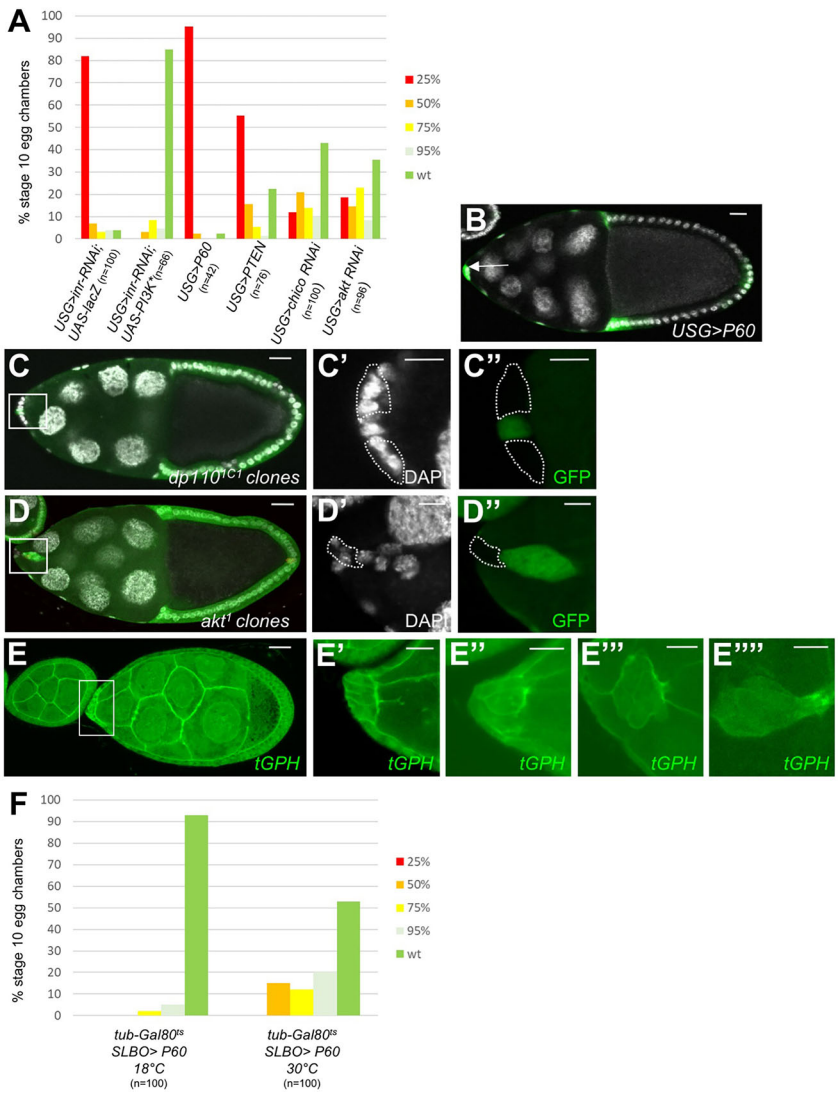

Fig. 2. The canonical IIS pathway is required for border cell migration. (A) Quantification of stage 10 border cell migration defects for each indicated genotype (classified as quartiles: 25%, clusters that have migrated to up to 25% of the distance; 50%, clusters that have migrated between 26 and 50% of the distance; 75%, clusters that have migrated between 51 and 75% of the distance; 95%, clusters that have migrated between 76 and 95% of the distance; wt, clusters that have reached the oocyte). (B) *USG>P60* stage 10A egg chambers showing an absence of border cell migration (border cells indicated by a white arrow). P60-expressing cells were identified by the presence of GFP. (C-C″) Mosaic cluster with $dp110^{1C1}$ mutant border cells, which remain attached to the anterior tip of a stage 10A egg chamber. White box in C outlines the border cells that are shown in C′-C″. (D-D″) Mosaic cluster for akt^{1} initiated the migration but remained attached to the anterior tip of an early stage 10A egg chamber. White box in D outlines the border cells that are shown in D′ and D″. (E-E″″) Visualisation of IIS/PI3K signalling by membrane localization of the *tGPH* reporter gene (green) in wild-type egg chambers. GPH is expressed in nurse cells, oocytes and follicle cells. GPH membrane accumulation is stronger in anterior follicle cells before border cell migration when compared with the adjacent follicle cells. (E′-E″″) High-magnification views of boxed region in E, indicating border cells expressing GPH during their migration. (F) Quantification of stage 10 border cell migration defects for $tubGal80^{ts}$*;SLBO>P60* flies raised at 18°C (restrictive temperature) or after a 3-4 h shift at 30°C (permissive temperature). (B-D) Nuclei were labelled using DAPI (grey). Mutant cells were identified by the absence of GFP and outlined with white dotted lines. Scale bars: 20 µm in B-E; 10 µm in C′-E″″.

0.53 µm/min, P60- and FoxO-expressing clusters showed reduced velocity with an average speed of 0.22 µm/min and 0.32 µm/min, respectively (Fig. 3J).

We next quantified protrusion features and dynamics from live egg chambers (Fig. 3G-M; Movies 4-6). Fig. 3G-I show still images extracted from 1 h movies from control (Movie 4), P60 (Movie 5) or FoxO-expressing (Movie 6) border cells. Results show that the number, length and lifetime of protrusions are all reduced in conditions of reduced IIS signalling. The average number of protrusions/h is 11.8 in control border cells, which is reduced to 6.8 and 7.6 in P60- and FoxO-expressing clusters, respectively (Fig. 3K). These limited protrusions also show a reduction in their average length, which is 5.56 µm for P60 and 4.74 µm for FoxO-expressing clusters, compared with 9.74 µm in control border cells (Fig. 3L). Finally, although the average lifetime of protrusions reaches 6.05 min in control border cells, it is reduced to 4.32 min and 4.38 min in P60 and FoxO-expressing clusters, respectively (Fig. 3M).

The actin cytoskeleton plays a crucial role for membrane ruffling and protrusion dynamics during border cell migration (Prasad and Montell, 2007). Interestingly, we observed that loss of *inr* function in follicle or border cells disrupted the polymerization of the actin cytoskeleton as shown by a strong reduction of F-actin structures (Fig. 4A-B′″″). Similarly, P60-expressing clusters also show a reduction of F-actin levels when compared with control (Fig. 4C-E). These findings suggest that the IIS pathway is important for the polymerization of the actin cytoskeleton and for the formation of dynamic protrusions that are essential for driving border cell delamination and migration.

The IIS pathway controls the levels of Profilin in follicle and border cells

Actin polymerization largely relies on the Profilin protein to maintain pools of monomeric actin. *Drosophila* Profilin is encoded by the *chickadee* (*chic*) gene, whose loss of function leads to border cell migration defects (Verheyen and Cooley, 1994).

Interestingly, we found that Profilin is ubiquitously expressed in egg chambers with a stronger accumulation in border cells throughout their migration (Fig. 5A,B; Fig. S2). Clonal analysis using the $chic^{D5203}$ mutation confirmed the importance of Profilin for the formation of F-actin structures and for border cell migration, which are both absent in mutant cells (Fig. 5C,D) (Verheyen and Cooley, 1994).

To test for a possible functional interaction between *chic*/Profilin and IIS, we performed genetic, molecular and rescue experiments. First, we observed that removing one functional copy of the *inr* gene led to a strong enhancement of a *chic* border cell migration

Development (2018) 145, dev161117. doi:10.1242/dev.161117

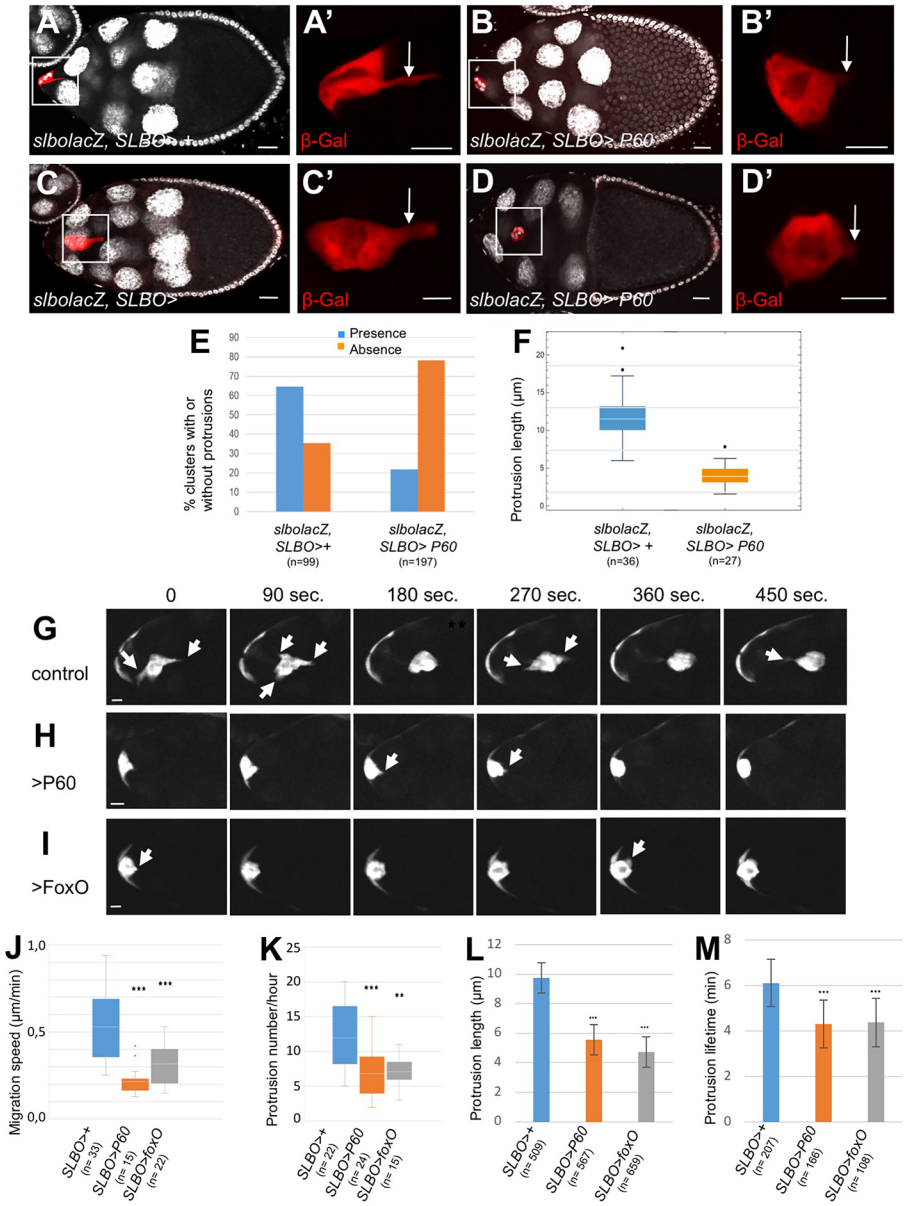

Fig. 3. The Insulin pathway controls the formation and dynamics of cell protrusions. (A-D) Late stage 9 egg chambers of control (A,C) and P60-expressing (B,D) border cells showing *slbo-lacZ* expression to reveal long cellular extensions (LCEs). In control, protrusions are visible before (A) and during (C) migration, whereas they are rarer and shorter in border cells overexpressing P60 (B,D). The boxed areas in A-D are shown in more detail in A′-D′, with only the β-galactosidase channel (red). White arrows indicate the protrusions. (E) Quantification of clusters with protrusions from control or P60-expressing stage 9 egg chambers. (F) Quantification of the length of protrusions from control or P60-expressing stage 9 egg chambers. Whisker plots with medians of 11.5 µm (control) and 3.9 µm (P60-expressing). (G-I) Single frames from Movies 4-6 showing migration and membrane protrusions from control (G), P60-expressing (H) and FoxO-expressing (I) border cells. (J) Quantification of migration speed from control (*Slbo*>+), *Slbo>P60* and *Slbo>FoxO* border cells. Whisker plots with medians of 0.53 µm/min (control), 0.22 µm/min (P60-expressing) and 0.32 µm/min (FoxO-expressing). Mann–Whitney test, ***P<0.001. (K) Quantification of protrusion numbers from control (*Slbo*>+), *Slbo>P60* and *Slbo>FoxO* border cells. Whisker plots with medians of 11.8 (control), 6.8 (P60-expressing) and 7.6 (FoxO-expressing). Mann–Whitney test, ***P<0.001, **P<0.01. (L) Quantification of protrusion length from control (*Slbo*>+), *Slbo>P60* and *Slbo>FoxO* border cells (***P<0.001). (M) Quantification of protrusion lifetime from control (*Slbo*>+), *Slbo>P60* and *Slbo>FoxO* border cells (***P<0.001). Scale bars: 20 µm in A-D; 10 µm in A′-D′,G-I.

phenotype. Although flies harbouring a heteroallelic combination for *chic* mutations ($chic^{1320}/chic^{D5203}$) had weak migration defects (13% of mutant egg chambers not migrating normally), the phenotype was greater than 50% when the flies were heterozygous for the inr^{ex15} mutation ($chic^{1320}/chic^{D5203}$; $inr^{ex15}/+$) (Fig. 5E,F).

Second, we found that IIS controls *chic* expression autonomously in both follicle and border cells, as shown by the strong reduction of Profilin protein accumulation in inr^{ex15} mutant cells (Fig. 5G-I). In addition, these mutant cells showed a strong reduction of a *chic-lacZ* reporter line (Fig. 5J,K), indicating that the IIS pathway controls *chic* expression transcriptionally.

Finally, we asked whether this activation of *chic* expression represents a major response to Insulin signalling during migration, by testing the ability of *chic* to rescue a loss of IIS activity. Interestingly, *chic* overexpression was able to rescue *inr-RNAi* border cell migration defects by a factor of 6.25 (frequency of normal border cell migration raising from 4% to greater than 25%; Fig. 5F). The partial phenotypic rescue suggests that IIS likely controls other processes that are necessary for full border cell migration, in addition to controlling Profilin accumulation. Taken together, these results show that IIS controls the levels of *chic*/Profilin expression, which in turn is important for specific and dynamic F-actin structures that are essential for the migration of border cells.

FoxO is a repressor of *chickadee* expression downstream of the IIS pathway

To further characterize the molecular mechanism controlling *chic* expression, we looked at the role of the FoxO transcription factor, the activity of which is inhibited by AKT downstream of IIS activation (Junger et al., 2003; Puig et al., 2003). We first generated mosaic border cells for the $foxo^{\Delta 94}$ amorphic allele and found that mutant clusters migrated normally (Fig. 6A-A″), thus indicating that *foxo* is dispensable for migration. However, overexpression of either a wild-type or a constitutively active nuclear form of FoxO (*UAS-hfoxO3a*; Junger et al., 2003) in border cells led to severe migration defects, with about 60% to 100% of clusters not migrating,

Development (2018) 145, dev161117. doi:10.1242/dev.161117

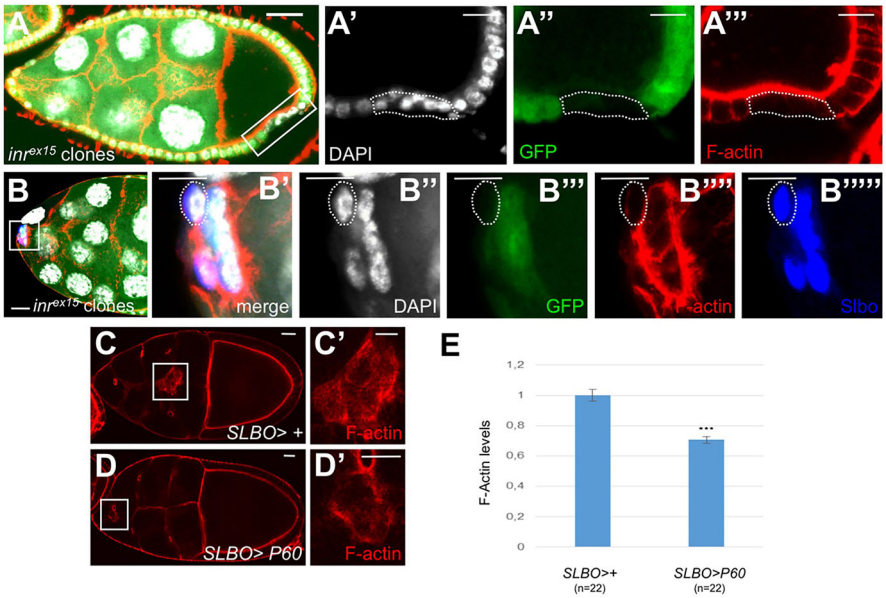

Fig. 4. The Insulin pathway controls the levels of F-actin. (A-A‴) High-magnification view of a *inr*^{ex15} mosaic stage 9 egg chamber showing a reduction of F-actin in mutant follicle cells. White box in A outlines the border cells that are shown in A′-A‴. (B‴′) High-magnification views of stage 10 *inr*^{ex15} mosaic cluster showing a reduction of F-actin in a mutant border cell. White box in B outlines the border cells that are shown in B′-B‴′. (C,C′) *slbo*>+ control egg chamber (late stage 9/early stage 10) stained with phalloidin (red). White box in C outlines the border cells that are shown in C′. (D,D′) *SLBO>P60* egg chamber (late stage 9/early stage 10) stained with phalloidin (red) shows delayed border cell migration and a reduction of F-actin in the cluster. White box in D outlines the border cells that are shown in D′. (E) Quantification of F-actin levels in control and P60-expressing clusters (***P<0.001). Data are mean±s.e.m. Egg chambers were stained for nuclei (A,B) (DAPI, grey), F-actin (A-D′) (rhodamine-phalloidin, red), Slbo (B) (blue) and GFP (A,B) (green). *inr*^{ex15} mutant cells were identified by the absence of GFP (A,B) and are outlined with white dotted lines. Scale bars: 20 µm in A-D; 10 µm in A′-D′.

respectively (Fig. 6B,C). These results clearly indicate that FoxO activity suppresses border cell migration.

To further assess whether FoxO controls cluster migration downstream of IIS, we generated clones of border cells that overexpressed the P60 subunit and that were also mutant for *foxo* (see Materials and Methods). The P60-induced border cell migration phenotype was suppressed in the absence of *foxo* (Fig. 6D), indicating that IIS downregulation prevents border cell migration through FoxO.

We next analysed FoxO protein expression and found that the protein is present in both germline and follicle cells during oogenesis (Fig. 6E-I). Interestingly, detailed analysis revealed a dynamic expression pattern of FoxO in border cells, as follows: (1) before or at early stage 8, FoxO expression is similar in presumptive border cells and surrounding follicle cells; (2) starting at the time of cluster formation (stage 8-9), during (late stage 9) and until the end of migration, FoxO levels decrease constantly and become visibly undetectable (Fig. 6F-I). Quantification of FoxO signal intensity (ratio between border and neighbouring follicle cells) at these four different stages reveal a gradual reduction of FoxO protein during cell migration (Fig. 6E). When the border cell cluster reaches the oocyte (stage 10), the relative amount of FoxO has dropped by about 70% of that of stage 8 levels (Fig. 6E). Of note, the dynamic pattern of FoxO expression well mirrors the pattern of IIS activity, as revealed by tGPH staining (Fig. 2E-E‴).

The decrease of FoxO and the concomitant increase of Profilin in border cells suggest that FoxO could negatively control *chic* expression to promote migration. To test this hypothesis further, we analysed the levels of *chic-lacZ* in border cells following FoxO overexpression and found that the levels of this reporter line were strongly reduced (Fig. 6J-M). Additionally, we analysed *chic* mRNA expression following *foxo* overexpression and found that the levels of *chic* transcripts were also strongly reduced (Fig. 6N). Altogether, these results show that IIS-mediated inhibition of FoxO at the onset of migration is essential to allow *chic* expression in border cells, thereby promoting the assembly of dynamic actin-rich protrusions necessary for cluster delamination and migration (Fig. 6O).

DISCUSSION

In this study, we identify the Insulin/IGF-Signalling (IIS) pathway as a key regulator of border cell migration during *Drosophila* oogenesis. We demonstrate that activation of InR at the onset of migration promotes actin dynamics in the outer border cells, the subpopulation of cells known to drive migration. In this process, the canonical IIS pathway is shown to act through the inhibition of the transcription factor FoxO, which leads to the de-repression of *chic*/*profilin*. High levels of Profilin in turn facilitate actin polymerization and the formation of dynamic protrusions and of specific, long actin cellular extensions that are required for delamination and proper migration of the invasive cell cluster (Fig. 6O).

The conserved IIS pathway couples nutritional cues with cellular metabolism, which in turn is essential for coordinating development with growth conditions. The systemic action of the IIS pathway thus makes it difficult to discriminate between chronic versus more acute or specific roles in particular cellular processes and during morphogenesis. In this context, border cells provide a powerful model with which to specifically address the role of the IIS pathway on cellular motility. During *Drosophila* oogenesis, the IIS pathway acts both in the germline and somatic cells to adjust egg chamber maturation rates to protein availability (Drummond-Barbosa and Spradling, 2001, 2004; Ikeya et al., 2002; Jouandin et al., 2014; LaFever, 2005). We show, using the FLP/FRT system, that chronic downregulation of IIS in border cells impairs their migration, a

Development (2018) 145, dev161117. doi:10.1242/dev.161117

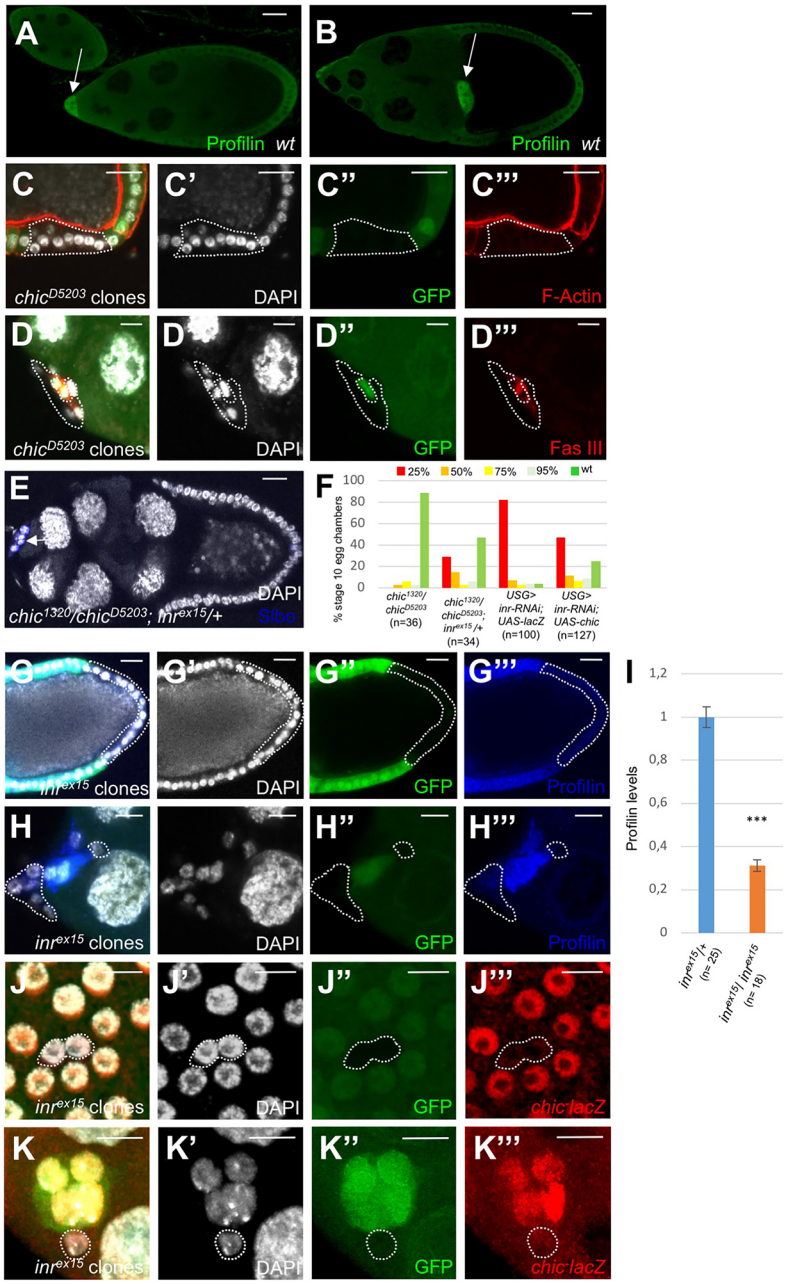

Fig. 5. The Insulin pathway controls the levels of Profilin in follicle and border cells. (A,B) Wild-type early stage 9 (A) and stage 10A (B) egg chambers stained using anti-Profilin antibodies. Profilin (green) is ubiquitously expressed but shows strong accumulation in border cells (indicated by white arrows) before and during their migration. (C-C′″) Stage 9 *chic*^{D5203} mosaic egg chamber stained with rhodamine-phalloidin (red) showed a reduction of F-actin in mutant follicle cells. (D-D′″) Mosaic cluster with *chic*^{D5203} mutant outer border cells and wild-type polar cells (indicated by Fas III staining, red) remained attached to the anterior tip of the egg chamber (stage 10A). (E) *chic*^{1320}/*chic*^{D5203}; *inr*^{ex15} /+ stage 10A egg chamber showing an absence of border cell migration, indicating a genetic interaction between *inr* and *chic*. Slbo (blue) labelled the border cells (white arrow). (F) Quantification of stage 10 border cell migration defects in *chic* and *inr* genetic combinations, showing dose-sensitive interaction between *chic* and *inr*, and a rescue of *inr-RNAi* migration defects by overexpression of Profilin in border cells (classified as quartiles: 25%, clusters that have migrated to up to 25% of the distance; 50%, clusters that have migrated between 26 and 50% of the distance; 75%, clusters that have migrated between 51 and 75% of the distance; 95%, clusters that have migrated between 76 and 95% of the distance; wt, clusters that have reached the oocyte). (G-G′″) *inr*^{ex15} mosaic egg chamber (stage 10A) showing a reduction in the level of Profilin (blue) in mutant follicle cells when compared with wild-type neighbouring cells. (H-H′″) High-magnification view of *inr*^{ex15} mosaic stage 10A egg chamber showing a reduction of Profilin (in blue) in mutant border cells. (I) Quantification of the Profilin signal in control and *inr*^{ex15} mutant cells (***P<0.001). Data are mean ±s.e.m. (J-K′″) Mosaic egg chambers (stage 10) with follicle cells (J-J′″) or border cells (K-K′″) mutant for *inr*^{ex15}. Mutant cells showed a strong reduction of *chic-lacZ* expression (red) when compared with neighbouring wild-type cells. *chic*^{D5203} and *inr*^{ex15} mutant cells were identified by the absence of the GFP clonal marker (C,D,G,H,J,K) and are outlined with white dotted lines (C,D,G,H,J,K). DAPI (grey) labelled nuclei (C-E,G-K). Scale bars: 20 µm in A-C′″,E,G-G′″; 10 µm in D-D′″,H-K′″.

process that can be associated with metabolic defects. Interestingly, our acute manipulation of IIS in border cells, using the Gal4/Gal80^{ts} system, shows that IIS downregulation can also block cluster migration specifically, a phenotype that can be rescued partly by restoring Profilin expression (Fig. 5). These data argue for an active control of cell migration by IIS, independently of cellular fitness. This view is consistent with previous work showing that in *ex vivo* experiments, Insulin-containing culture medium is necessary to support egg chamber development and border cell migration (Bianco et al., 2007; Prasad and Montell, 2007).

Border cells migrate towards the oocyte to make the micropyle: an opening that allows oocyte fertilization through the chorion. In this process, border cell migration needs to be synchronized with oocyte growth. We propose that the dual role of IIS for both egg chamber growth and border cell migration could help to coordinate migratory events with organ maturation, thereby ensuring the robust morphogenesis that is important for fertility.

Actin dynamics are essential to a multitude of cellular and morphogenetic processes; therefore, understanding the diverse modes of actin regulation is of prime interest. Members of the IIS pathway have been linked to actin regulation in a number of normal and pathological processes (Xue and Hemmings, 2013). For example, IIS plays an important role in neuronal guidance (Liu et al., 2014; Song, 2003) or wound healing (Kakanj et al., 2016). Additionally, PI3K has been shown to couple glycolytic flux with actin dynamics (Hu et al., 2016), whereas AKT participates in the epithelial-to-mesenchymal transition required to drive mesoderm formation during gastrulation (Montero et al., 2003; Yang et al., 2008). Accumulating evidence also indicates that PI3K/AKT controls the migratory phenotype of metastatic cells (Xue and Hemmings, 2013). In breast cancer cells, AKT enhances cell migration and invasion through increased filopodia formation, which can be blocked with a specific AKT inhibitor (Yang et al., 2004). These observations suggest a model in which AKT

Development (2018) 145, dev161117. doi:10.1242/dev.161117

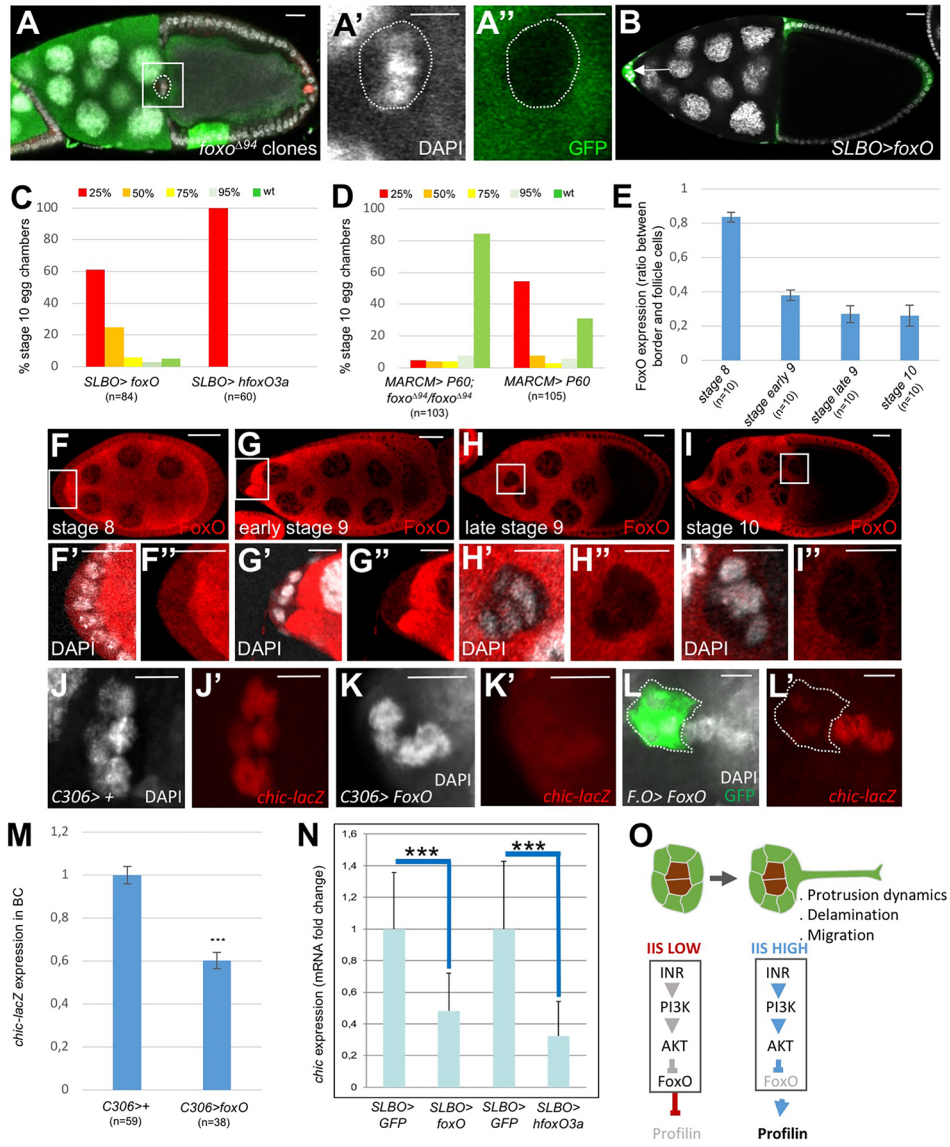

Fig. 6. FoxO is a repressor of *chickadee*/Profilin expression downstream of the Insulin pathway. (A) Mosaic *foxo*$^{\Delta 94}$ egg chamber (stage 10A) showing a mutant cluster migrating normally. *foxo*$^{\Delta 94}$ mutant cells were identified by the absence of the GFP clonal marker (green) and are outlined with white dotted lines. White box showing border cells in A is enlarged in A′,A″. (B) Overexpression in a stage 10A egg chamber of a wild-type form of FoxO impaired border cell migration (border cells are indicated by a white arrow). FoxO-overexpressing cells were identified by the presence of GFP. (C) Quantification of border cell migration defects from stage 10 egg chambers overexpressing FoxO or an activated form of FoxO (hFoxO3a). (D) Quantification of border cell migration defects from stage 10 egg chambers expressing P60, in absence or in presence of *foxo*. 25%, clusters that have migrated to up to 25% of the distance; 50%, clusters that have migrated between 26 and 50% of the distance; 75%, clusters that have migrated between 51 and 75% of the distance; 95%, clusters that have migrated between 76 and 95% of the distance; wt, clusters that have reached the oocyte. (E) Quantification, from stage 8 to stage 10, of FoxO protein levels in border cells of wild-type egg chambers, shown as normalized intensity with respect to neighbouring follicle cells. Error bars represent s.e.m. (F-I) Decreasing expression of FoxO (stained with anti-FoxO antibodies; red) in wild-type egg chambers from stage 8 to stage 10. (F′,F″,G′,G″,H′,H″,I′,I″) Enlargements of the border cells boxed in F-I. (J-K′) Expression of *chic-lacZ* in control (J,J′) and FoxO-expressing (K-K′) border cell clusters. Images show a high-magnification view of border cells from stage 10A egg chambers. (L,L′) Expression of *chic-lacZ* in a mosaic border cell cluster overexpressing FoxO (GFP-positive cells). (M) Quantification of *chic-lacZ* expression from control (*c306>)* and *c306>FoxO* border cell clusters (***P<0.001). Representative samples are shown in J-K′. (N) *chic* expression is repressed following FoxO expression. Quantification of *chic* expression (qRT-PCR from total ovaries) from control (*SLBO>GFP*), *SLBO>foxo* and *SLBO>hfoxo3a* flies. Fold changes are relative to the control condition. Data represent the mean of triplicate experiments±s.d. (***P<0.005). (O) Model for the role of the IIS pathway in regulating actin dynamics, protrusion formation and border cell migration. At early stages, IIS is low in the outer border cells and Profilin is expressed at basal levels. Starting at early stage 9, the high IIS activation leads to strong Profilin expression, allowing LCE formation and protrusion dynamics required for delamination and subsequent migration of the cluster. Scale bars: 20 µm in A,B,F-I; 10 µm in A′,A″,F′-L′.

activation potentially influences cell motility through direct modulation of actin, which is supported by studies showing that actin preferentially binds to phosphorylated AKT at pseudopodia sites (Amiri et al., 2007; Cenni et al., 2003). Despite this evidence, the view is fragmented and data are lacking that demonstrate a clear role for the full canonical pathway in cytoskeleton plasticity. In particular, the requirement of IIS transcriptional regulation in this process remained elusive. In this report, we reveal that canonical IIS acts through inhibition of the transcription factor FoxO to control a major actin regulator: Profilin. These data reveal a molecular

Development (2018) 145, dev161117. doi:10.1242/dev.161117

mechanism for FoxO-mediated control of actin remodelling, which may be generalized to other processes where actin dynamics is particularly important. For example, during wound healing in *Drosophila* larvae, formation of an acto-myosin cable has been shown to depend on PI3K activation and redistribution of the transcription factor FoxO (Kakanj et al., 2016).

In conclusion, our findings establish the canonical IIS pathway as a gene regulatory network important for collective cell migration (Sharma et al., 2018). The data also identify a novel mechanism by which actin homeostasis and organization is regulated transcriptionally in a dynamic migratory process. By this mechanism, the formation of actin-rich protrusions is constitutively and negatively controlled by the transcription factor FoxO, the inhibition of which by IIS signalling can generate peak levels of actin polymerization required for delamination and migration. It will be interesting to establish whether the control of Profilin expression through IIS signalling represents a general mechanism that controls actin remodelling in cell and tissue morphogenesis.

MATERIALS AND METHODS

Drosophila strains and genetics

Drosophila culture and crosses were performed following standard procedures at 25°C, except where indicated. The following *Drosophila* strains were used: *inr-RNAi* (National Institute of Genetics, NIG-Fly); *akt-RNAi* and *chico-RNAi* (VDRC, Vienna Drosophila Resource Center) (Dietzl et al., 2007); *UAS-foxo* and *UAS-dp110^{CAAX}* (Bloomington); *slbo-Gal4* (Rørth et al., 1998); *upd-Gal4* and *slbo-Gal4, UAS-mCD8 GFP* (a gift from D. Montell, University of California, Santa Barbara, USA); *slbo-Gal4, tGPH* and *slbo-Gal4, slbo-flac* (referred to as *slbo-lacZ*) (Fulga and Rørth, 2002); *UAS-hfoxO3a* (Junger et al., 2003); *chic^{D5203}FRT40A*, *chic^{1320}* and *UAS-chic* (a gift from L. Cooley, Yale University, New Haven, USA); *UAS-P60, UAS-PTEN* (a gift from P. Léopold, Institut de Biologie Valrose, Nice, France); *inr^{ex15} FRT82B* (Song, 2003) (a gift from L. Pick, University of Maryland, USA); *dp110^{1C1}FRT82B* (a gift from H. Stöcker, ETH, Zurich, Switzerland; Willecke et al., 2011); *foxO$^{\Delta 94}$ FRT82B* (Slack et al., 2011); and *akt^{1} FRT82B* (Rintelen et al., 2001).

For expression induced using the Gal4/UAS system, 2-day-old females with the designated genotypes were incubated for 2 days at 29°C before dissection. *w^{1118}* flies were used as control.

Generation of mosaic clones

Mutant follicle cell clones were generated by mitotic recombination using the FLP/FRT technique (Xu and Rubin, 1993). Flies with mutations on *FRT82B* chromosomes were crossed with *hsFLP;; FRT82B, UbiGFP* flies. *chic^{D5203}FRT40A* flies were crossed with *hsFLP; FRT40A, UbiGFP* flies.

UAS-P60; FRT82B foxo$^{\Delta 94}$ and *UAS-P60; FRT82B* flies were crossed with *yw, tubGal4-UAS GFP; FRT82B, tub Gal80^{ts}* flies (a gift from A. Ephrussi, EMBL, Heidelberg, Germany) to generate MARCM clones (Lee and Luo, 1999).

Mosaic clones were generated as follows: females with the required genotypes were heat-shocked for 1 h at 37°C, twice a day for 3 days and dissected 2 days later. Mosaic mutant clones were marked by the absence (FLP/FRT) or by the presence of GFP (MARCM).

Flip-out clones were made from *UAS-foxO* flies crossed to hsFLP;; act<CD2>GAL4, UAS-GFP (a gift from D. Montell). The progeny was heat-shocked for 1 h at 37°C and dissected 2 days later.

TARGET system

Conditional expression of *UAS-P60* was achieved using the TARGET system (McGuire, 2003), combining the UAS/Gal4 bipartite expression system with a thermosensitive form of the Gal4 negative regulator, Gal80^{ts}, to switch on and off expression of the UAS-construct at desired developmental time points.

Briefly, the *tub-Gal80^{ts}; slbo-GAL4>P60* flies were obtained and raised at 18°C for 1 day. At this restrictive temperature, Gal80^{ts} is active and blocks Gal4 function, leading to an absence of *UAS-P60* expression. Flies were then raised for 3-4 h at permissive temperature (30°C), leading to Gal80^{ts} inactivation and hence allowing Gal4 to activate *UAS-P60* expression and consequently IIS pathway inhibition in border cells. Flies were dissected immediately after temperature shifts.

UAS-RNAi screen

This screen was performed by crossing the NIG-Fly *UAS-RNAi* transgenic fly collection with the *USG>* driver (a combination of *UPD>* and *SLBO>*), which allows the targeted expression of *UAS* constructs in both polar and outer border cells, together with a *UAS-GFP* transgene allowing the visualization of the border cell cluster (De Graeve et al., 2012). *USG>UAS-RNAi* females were dissected after 2 days of incubation at 29°C, and candidate *UAS-RNAi* lines were selected when abnormal border cell migration was observed in more than 20% of stage 10 egg chambers.

Immunostaining and imaging

Ovary dissection, fixation and staining with antibodies, phalloidin and DAPI were performed as described previously (Devergne et al., 2007; Ghiglione et al., 2008). The primary antibodies used were: rabbit anti-Slbo (1:1000; De Graeve et al., 2012); mouse anti-Singed [1:50, SN7C, Developmental Studies Hybridoma Bank (DSHB), University of Iowa, USA]; mouse anti-FasIII (1:100, 7G10, DSHB); mouse anti-Profilin (1:100, DSHB); rabbit anti-FoxO (1:500; Shin et al., 2011; Slaidina et al., 2009); and chicken anti-β-Galactosidase (1:1000, Gene Tex).

Alexa Fluor-conjugated goat antibodies were used as secondary antibodies (Molecular Probes). Phalloidin conjugates and DAPI (1:1000, Sigma) were used to outline cells and label DNA, respectively. The samples were mounted in Mowiol and images were taken on a Zeiss LSM510 or LSM710 confocal microscope. Quantification of protrusion length was performed using the ImageJ software.

Time-lapse microscopy

Imaging of live border cell migration was performed using an Olympus spinning-disc confocal microscope (20×objective+1.5×lens) coupled with an Andor camera. Acquisition was carried out using Metamorph software. Egg chambers were cultured in S2 culture medium with 1 µg/ml Insulin at 22°C and processed as described previously (Prasad and Montell, 2007). Movies were captured over a period of 1 h (1.30 min. interval) or 8 h (10 min. interval). Cluster velocity and protrusion length, frequency and dynamics were analysed on *Slbo-Gal4>UAS-CD8::GFP* (control) and *Slbo-Gal4>UAS-CD8::GFP>UAS-P60* or *Slbo-Gal4>UAS-CD8::GFP>UAS-FoxO* flies. Analysis was carried out using ImageJ software.

Real-time RT-PCR

Total RNA extraction from dissected ovaries and real-time RT-PCR for *chickadee* were performed as previously described (Slaidina et al., 2009). Three independent biological experiments each with a triplicate measurement were conducted. Primers (left 5′-ctgcatgaagacaacacaagc-3′ and right 5′-caagtttctctaccacggaagc-3′) were designed using the Primer Express software (Applied Biosystems) and tested by standard curve experiments.

Acknowledgements

We thank all members of S.N.'s laboratory for fruitful discussions; members of P. Léopold's laboratory for providing numerous reagents and helpful advice; A. Popkova for teaching us time-lapse imaging of egg chambers in culture; L. Cooley, A. Ephrussi, P. Gallant, E. Hafen, D. Montell, W. J. Lee, L. Partridge, L. Pick, P. Rorth and H. Stöcker for reagents; the DSHB for antibodies; the Bloomington Drosophila Stock Center, the National Institute of Genetics Fly (NIG-Fly) and Vienna Drosophila RNAi Center (VDRC) for providing *Drosophila* fly lines. We thank F. Bondi, D. Chobert, F. De Graeve, M. A. Derieppe, G. Gozzerino, L. Parel, M. Pierret, A. Samuel and J. Soltys for their help with the UAS-RNAi screen; and the iBV PRISM platform for providing state of the art imaging resources and advice. Some data are reproduced from P.J.'s PhD thesis, defended at Institut de Biologie Valrose in 2013.

Competing interests

The authors declare no competing or financial interests.

Author contributions
Conceptualization: C.G., P.J., S.N.; Methodology: C.G.; Validation: C.G., P.J.; Formal analysis: C.G., P.J.; Investigation: C.G., P.J.; Resources: D.C.; Data curation: D.C.; Writing - original draft: S.N.; Writing - review & editing: C.G., P.J., S.N.; Supervision: C.G., S.N.; Project administration: S.N.; Funding acquisition: S.N.

Funding
Work in S.N.'s laboratory is supported by the Université Côte d'Azur, the Centre National pour la Recherche Scientifique, the Université Nice Sophia Antipolis, the Institut National de la Santé et de la Recherche Médicale, the Agence Nationale pour la Recherche and LABEX SIGNALIFE (ANR-11-LABX-0028-01).

Supplementary information
Supplementary information available online at
http://dev.biologists.org/lookup/doi/10.1242/dev.161117.supplemental

References

Amiri, A., Noei, F., Jeganathan, S., Kulkarni, G., Pinke, D. E. and Lee, J. M. (2007). eEF1A2 activates Akt and stimulates Akt-dependent actin remodeling, invasion and migration. *Oncogene* **26**, 3027-3040.
Andersen, D. S., Colombani, J. and Léopold, P. (2013). Coordination of organ growth: Principles and outstanding questions from the world of insects. *Trends Cell Biol.* **23**, 336-344.
Beccari, S., Teixeira, L. and Rørth, P. (2002). The JAK/STAT pathway is required for border cell migration during Drosophila oogenesis. *Mech. Dev.* **111**, 115-123.
Bianco, A., Poukkula, M., Cliffe, A., Mathieu, J., Luque, C. M., Fulga, T. A. and Rørth, P. (2007). Two distinct modes of guidance signalling during collective migration of border cells. *Nature* **448**, 362-365.
Borghese, L., Fletcher, G., Mathieu, J., Atzberger, A., Eades, W. C., Cagan, R. L. and Rørth, P. (2006). Systematic analysis of the transcriptional switch inducing migration of border cells. *Dev. Cell* **10**, 497-508.
Britton, J. S., Lockwood, W. K., Li, L., Cohen, S. M. and Edgar, B. A. (2002). Drosophila's insulin/PI3-kinase pathway coordinates cellular metabolism with nutritional conditions. *Dev. Cell* **2**, 239-249.
Cenni, V., Sirri, A., Riccio, M., Lattanzi, G., Santi, S., de Pol, A., Maraldi, N. M. and Marmiroli, S. (2003). Targeting of the Akt/PKB kinase to the actin skeleton. *Cell. Mol. Life Sci.* **60**, 2710-2720.
Colombié, N., Choesmel-Cadamuro, V., Series, J., Emery, G., Wang, X. and Ramel, D. (2017). Non-autonomous role of Cdc42 in cell-cell communication during collective migration. *Dev. Biol.* **423**, 12-18.
De Graeve, F. M., Van de Bor, V., Ghiglione, C., Cerezo, D., Jouandin, P., Ueda, R., Shashidhara, L. S. and Noselli, S. (2012). Drosophila apc regulates delamination of invasive epithelial clusters. *Dev. Biol.* **368**, 76-85.
Devergne, O., Ghiglione, C. and Noselli, S. (2007). The endocytic control of JAK/STAT signalling in Drosophila. *J. Cell Sci.* **120**, 3457-3464.
Dietzl, G., Chen, D., Schnorrer, F., Su, K.-C., Barinova, Y., Fellner, M., Gasser, B., Kinsey, K., Oppel, S., Scheiblauer, S. et al. (2007). A genome-wide transgenic RNAi library for conditional gene inactivation in Drosophila. *Nature* **448**, 151-156.
Drummond-Barbosa, D. and Spradling, A. C. (2001). Stem cells and their progeny respond to nutritional changes during Drosophila oogenesis. *Dev. Biol.* **231**, 265-278.
Drummond-Barbosa, D. and Spradling, A. C. (2004). α-Endosulfine, a potential regulator of insulin secretion, is required for adult tissue growth control in Drosophila. *Dev. Biol.* **266**, 310-321.
Duchek, P. and Rorth, P. (2001). Guidance of cell migration by EGF receptor signaling during Drosophila oogenesis. *Science* **291**, 131-133.
Duchek, P., Somogyi, K., Jékely, G., Beccari, S. and Rørth, P. (2001). Guidance of cell migration by the Drosophila PDGF/VEGF receptor. *Cell* **107**, 17-26.
Edgar, B. A. (2006). How flies get their size: genetics meets physiology. *Nat. Rev. Genet.* **7**, 907-916.
Fernandez-Almonacid, R. and Rosen, O. M. (1987). Structure and ligand specificity of the Drosophila melanogaster insulin receptor. *Mol. Cell. Biol.* **7**, 2718-2727.
Fulga, T. A. and Rørth, P. (2002). Invasive cell migration is initiated by guided growth of long cellular extensions. *Nat. Cell Biol.* **4**, 715-719.
Ghiglione, C., Devergne, O., Georgenthum, E., Carballès, F., Médioni, C., Cerezo, D. and Noselli, S. (2002). The Drosophila cytokine receptor Domeless controls border cell migration and epithelial polarization during oogenesis. *Development* **129**, 5437-5447.
Ghiglione, C., Devergne, O., Cerezo, D. and Noselli, S. (2008). Drosophila RalA is essential for the maintenance of Jak/Stat signalling in ovarian follicles. *EMBO Rep.* **9**, 676-682.
Hu, H., Juvekar, A., Lyssiotis, C. A., Lien, E. C., Albeck, J. G., Oh, D., Varma, G., Hung, Y. P., Ullas, S., Lauring, J. et al. (2016). Phosphoinositide 3-kinase regulates glycolysis through mobilization of aldolase from the actin cytoskeleton. *Cell* **164**, 433-446.
Ikeya, T., Galic, M., Belawat, P., Nairz, K. and Hafen, E. (2002). Nutrient-dependent expression of insulin-like peptides from neuroendocrine cells in the CNS contributes to growth regulation in Drosophila. *Curr. Biol.* **12**, 1293-1300.
Jang, A. C.-C., Chang, Y.-C., Bai, J. and Montell, D. (2009). Border-cell migration requires integration of spatial and temporal signals by the BTB protein Abrupt. *Nat. Cell Biol.* **11**, 569-579.
Jouandin, P., Ghiglione, C. and Noselli, S. (2014). Starvation induces FoxO-dependent mitotic-to-endocycle switch pausing during Drosophila oogenesis. *Development* **141**, 3013-3021.
Junger, M. A., Rintelen, F., Stocker, H., Wasserman, J. D., Végh, M., Radimerski, T., Greenberg, M. E. and Hafen, E. (2003). The Drosophila forkhead transcription factor FOXO mediates the reduction in cell number associated with reduced insulin signaling. *J. Biol.* **2**, 20.
Kakanj, P., Moussian, B., Grönke, S., Bustos, V., Eming, S. A., Partridge, L. and Leptin, M. (2016). Insulin and TOR signal in parallel through FOXO and S6K to promote epithelial wound healing. *Nat. Commun.* **7**, 12972.
LaFever, L. (2005). Direct control of germline stem cell division and cyst growth by neural insulin in Drosophila. *Science* **309**, 1071-1073.
LaFever, L., Feoktistov, A., Hsu, H.-J. and Drummond-Barbosa, D. (2010). Specific roles of Target of rapamycin in the control of stem cells and their progeny in the Drosophila ovary. *Development* **137**, 2451-2451.
Lee, T. and Luo, L. (1999). Mosaic analysis with a repressible cell marker for studies of gene function in neuronal morphogenesis. *Neuron* **22**, 451-461.
Liu, J., Spéder, P. and Brand, A. H. (2014). Control of brain development and homeostasis by local and systemic insulin signalling. *Diabetes Obes. Metab.* **16**, 16-20.
McDonald, J. A., Pinheiro, E. M., Kadlec, L., Schupbach, T. and Montell, D. J. (2006). Multiple EGFR ligands participate in guiding migrating border cells. *Dev. Biol.* **296**, 94-103.
McGuire, S. E. (2003). Spatiotemporal rescue of memory dysfunction in Drosophila. *Science* **302**, 1765-1768.
Montell, D. J. (2003). Border-cell migration: the race is on. *Nat. Rev. Mol. Cell Biol.* **4**, 13-24.
Montell, D. J. (2006). The social lives of migrating cells in Drosophila. *Curr. Opin. Genet. Dev.* **16**, 374-383.
Montell, D. J., Rorth, P. and Spradling, A. C. (1992). *Slow border cells*, a locus required for a developmentally regulated cell migration during oogenesis, encodes *Drosophila* C/EBP. *Cell* **71**, 51-62.
Montero, J.-A., Kilian, B., Chan, J., Bayliss, P. E. and Heisenberg, C.-P. (2003). Phosphoinositide 3-Kinase is required for process outgrowth and cell polarization of gastrulating mesendodermal cells. *Curr. Biol.* **13**, 1279-1289.
Petruzzelli, L., Herrera, R., Arenas-Garcia, R., Fernandez, R., Birnbaum, M. J. and Rosen, O. M. (1986). Isolation of a Drosophila genomic sequence homologous to the kinase domain of the human insulin receptor and detection of the phosphorylated Drosophila receptor with an anti-peptide antibody. *Proc. Natl. Acad. Sci. USA* **83**, 4710-4714.
Prasad, M. and Montell, D. J. (2007). Cellular and molecular mechanisms of border cell migration analyzed using time-lapse live-cell imaging. *Dev. Cell* **12**, 997-1005.
Puig, O., Marr, M. T. M., Ruhf, M. L. and Tjian, R. (2003). Control of cell number by Drosophila FOXO : downstream and feedback regulation of the insulin receptor pathway. *Genes Dev.* **17**, 2006-2020.
Ridley, A. J. (2003). Cell migration: integrating signals from front to back. *Science* **302**, 1704-1709.
Rintelen, F., Stocker, H., Thomas, G. and Hafen, E. (2001). PDK1 regulates growth through Akt and S6K in Drosophila. *Proc. Natl. Acad. Sci. USA* **98**, 15020-15025.
Rorth, P. (2009). Collective cell migration. *Annu. Rev. Cell Dev. Biol.* **25**, 407-429.
Rørth, P., Szabo, K., Bailey, A., Laverty, T., Rehm, J., Rubin, G. M., Weigmann, K., Milán, M., Benes, V., Ansorge, W. et al. (1998). Systematic gain-of-function genetics in Drosophila. *Development* **125**, 1049-1057.
Sharma, A., Halder, S., Felix, M., Nisaa, K., Deshpande, G. and Prasad, M. (2018). Insulin signaling modulates border cell movement in Drosophila oogenesis. *Development* **145**, dev166165 (in press).
Shin, S. C., Kim, S.-H., You, H., Kim, B., Kim, A. C., Lee, K.-A., Yoon, J.-H., Ryu, J.-H. and Lee, W.-J. (2011). Drosophila microbiome modulates host developmental and metabolic homeostasis via insulin signaling. *Science* **334**, 670-674.
Silver, D. L. and Montell, D. J. (2001). Paracrine signaling through the JAK/STAT pathway activates invasive behavior of ovarian epithelial cells in drosophila. *Cell* **107**, 831-841.
Slack, C., Giannakou, M. E., Foley, A., Goss, M. and Partridge, L. (2011). dFOXO-independent effects of reduced insulin-like signaling in Drosophila. *Aging Cell* **10**, 735-748.
Slaidina, M., Delanoue, R., Gronke, S., Partridge, L. and Léopold, P. (2009). A Drosophila insulin-like peptide promotes growth during nonfeeding states. *Dev. Cell* **17**, 874-884.
Song, J., Wu, L., Chen, Z., Kohanski, R. A. and Pick, L. (2003). Axons guided by insulin receptor in drosophila visual system. *Science* **300**, 502-505.
Van de Bor, V., Zimniak, G., Cerezo, D., Schaub, S., Noselli, S., Cérézo, D., Schaub, S. and Noselli, S. (2011). Asymmetric localisation of cytokine mRNA is

essential for JAK/STAT activation during cell invasiveness. *Development* **138**, 1383-1393.

Verheyen, E. M. and Cooley, L. (1994). Profilin mutations disrupt multiple actin-dependent processes during Drosophila development. *Development* **120**, 717-728.

Wang, X., Bo, J., Bridges, T., Dugan, K. D., Pan, T., Chodosh, L. A. and Montell, D. J. (2006). Analysis of cell migration using whole-genome expression profiling of migratory cells in the Drosophila ovary. *Dev. Cell* **10**, 483-495.

Weinkove, D., Neufeld, T. P., Twardzik, T., Waterfield, M. D. and Leevers, S. J. (1999). Regulation of imaginal disc cell size, cell number and organ size by Drosophila class I(A) phosphoinositide 3-kinase and its adaptor. *Curr. Biol.* **9**, 1019-1029.

Willecke, M., Toggweiler, J. and Basler, K. (2011). Loss of PI3K blocks cell-cycle progression in a Drosophila tumor model. *Oncogene* **30**, 4067-4074.

Xu, T. and Rubin, G. M. (1993). Analysis of genetic mosaics in developing and adult Drosophila tissues. *Development* **117**, 1223-1237.

Xue, G. and Hemmings, B. A. (2013). PKB/akt-dependent regulation of cell motility. *J. Natl. Cancer Inst.* **105**, 393-404.

Yang, L., Dan, H. C., Sun, M., Liu, Q., Sun, X.-M., Feldman, R. I., Hamilton, A. D., Polokoff, M., Nicosia, S. V., Herlyn, M. et al. (2004). Akt/protein kinase B signaling inhibitor-2, a selective small molecule inhibitor of Akt signaling with antitumor activity in cancer cells overexpressing Akt. *Cancer Res.* **64**, 4394-4399.

Yang, X., Chrisman, H. and Weijer, C. J. (2008). PDGF signalling controls the migration of mesoderm cells during chick gastrulation by regulating N-cadherin expression. *Development* **135**, 3521-3530.

Supplemental Figure S1 (related to Figure 1): Singed is expressed normally in *dinr*^{ex15} mutant border cells

A-A’’’, Expression of Singed in control cells from a stage 10A egg chamber.

B-B’’’, **C-C’’’**, Expression of Singed is not affected in *dinr*^{ex15} mutant border cells (stage 10A) as compared to wild type (**A, A’’’**). Mutant clusters did not migrated (**B-B’’’**) or migrated when 2 border cells were mutant (**C-C’’’**). Mutant cells are identified by the absence of the GFP clonal marker and outlined with white dotted lines.

D, Quantification of the Singed signal in control and *dinr*^{ex15} mutant border cells (n.s., not significant).

A-C, White boxes showing border cells are enlarged in **A’-A’’’**, **B’-B’’’**, **C’-C’’’**.

Nuclei are labelled with DAPI, grey; GFP, green; Singed, red.

Scale bars, 20 μm in (**A-C**), 10 μm in (**A’-C’’’**).

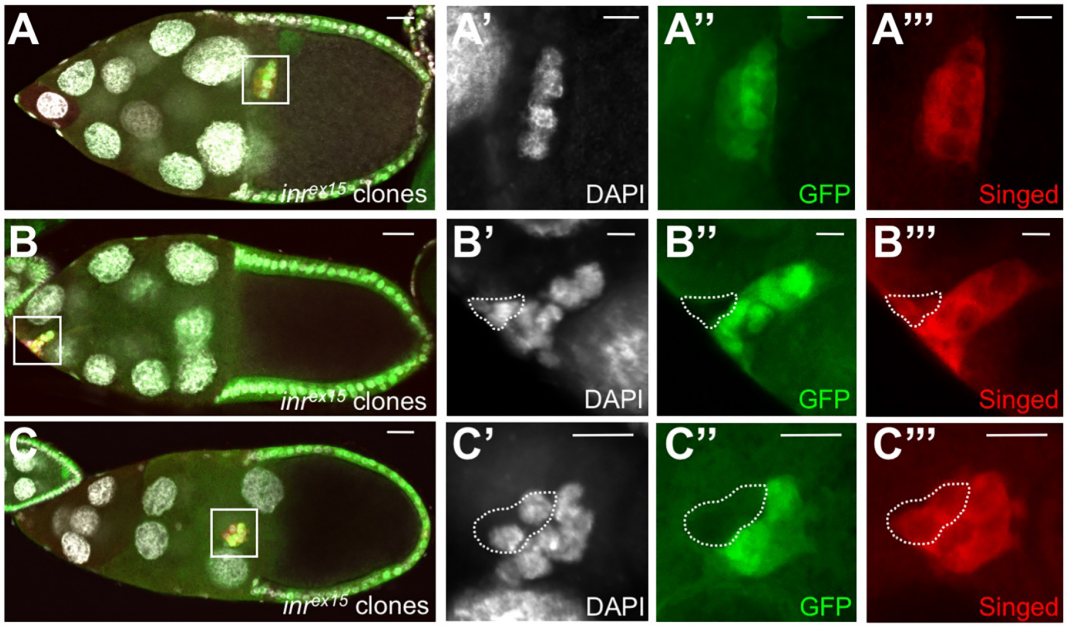

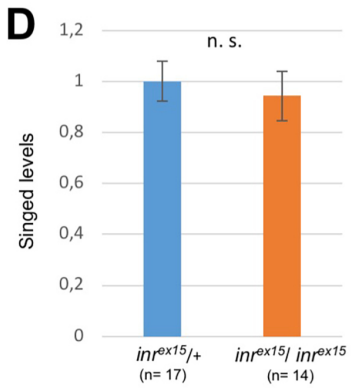

Figure S1

Supplemental Figure S2 (related to Figure 5): Specificity of the anti-Profilin antibodies.

A-A''', *chic*^{D5203} mosaic egg chamber (stage 10A) stained with anti-Profilin antibodies showing a strong reduction of the signal (in red), as compared to wildtype neighboring cells. Mutant cells are identified by the absence of the GFP clonal marker and outlined with white dotted lines.

B-B''', A stage 10A egg chamber overexpressing Profilin (*slbo-Gal4, UAS-GFP; UAS-chic*) shows a strong accumulation of the Profilin signal (in red) in border cells as well as anterior and polar posterior follicle cells reflecting *slbo-Gal4* expression pattern (in green). Note the normal migration of border cells despite overexpression of Profilin.

C, Quantification of the Profilin signal in control and *chic*^{D5203} mutant border cells (***p<0.001).

Scale bars, 20 μm.

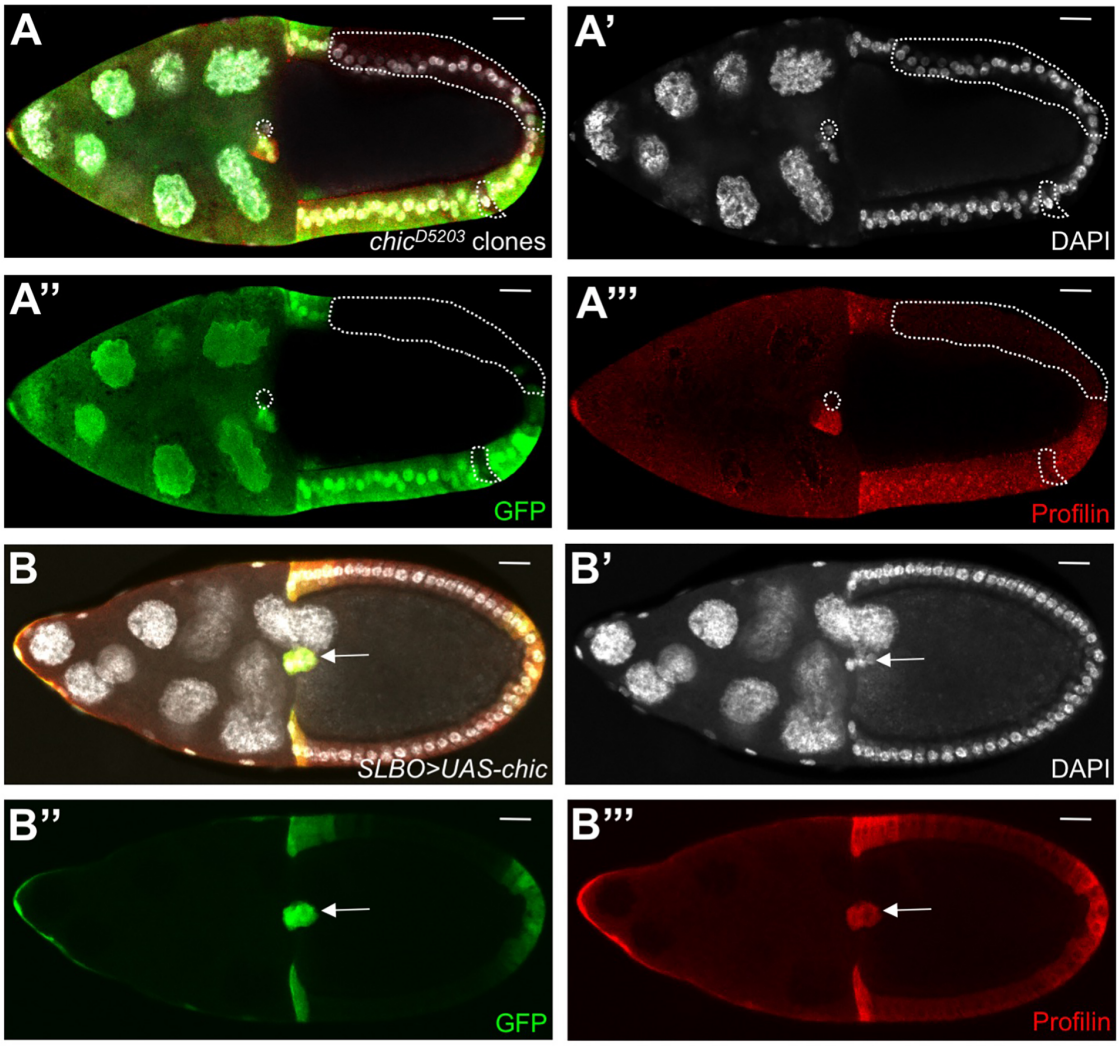

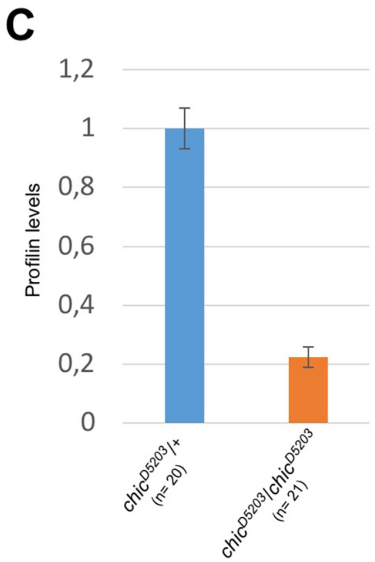

Figure S2

Movie 1 (related to Fig. 3): Time-lapse movie (8 hours, 10 min. intervals) showing the migration of control border cells (*slbo-Gal4, UAS-mCD8::GFP*).

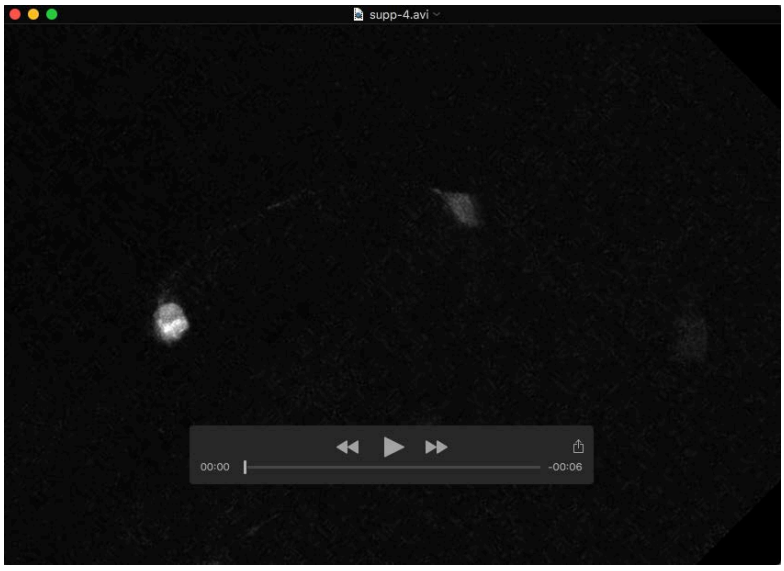

Movie 2 (related to Fig. 3): Time-lapse movie (8 hours, 10 min. intervals) showing the migration of border cells expressing P60 (*slbo-Gal4, UAS-mCD8::GFP; UAS-P60*).

Movie 3 (related to Fig. 3): Time-lapse movie (8 hours, 10 min. intervals) showing the migration of border cells expressing FoxO (*slbo-Gal4, UAS-mCD8::GFP; UAS-FoxO*).

Movie 4 (related to Fig. 3): Time-lapse movie (1 hour, 90 sec. intervals) showing the number, length and dynamics of protrusions from control border cells (*slbo-Gal4, UAS-mCD8::GFP*).

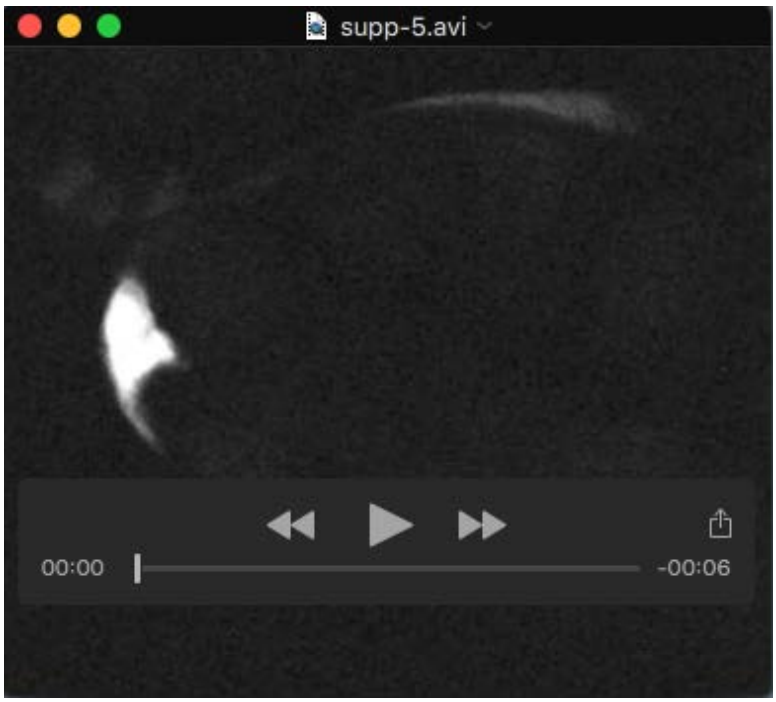

Movie 5 (related to Fig. 3): Time-lapse movie (1 hour, 90 sec. intervals) showing reduced number, length and dynamics of protrusions from border cells expressing P60 (*slbo-Gal4, UAS-mCD8::GFP; UAS-P60*).

Movie 6 (related to Fig. 3): Time-lapse movie (1 hour, 90 sec. intervals) showing reduced number, length and dynamics of protrusions from border cells expressing FoxO (*slbo-Gal4, UAS-mCD8::GFP; UAS-FoxO*).